

# Pressure-driven semiconductor-semiconductor transition and its structural origin in oxygen vacancy ordered $\text{SrCoO}_{2.5}$

Fang Hong,<sup>1,2</sup> Binbin Yue,<sup>1,2,\*</sup> Zhenxian Liu,<sup>3</sup> Bin Chen,<sup>1,†</sup> and Ho-Kwang Mao<sup>1,3</sup><sup>1</sup>*Center for High Pressure Science and Technology Advanced Research, 1690 Cailun Road, Pudong, Shanghai 201203, People's Republic of China*<sup>2</sup>*Advanced Light Source, Lawrence Berkeley National Laboratory, Berkeley, California 94720, USA*<sup>3</sup>*Geophysical Laboratory, Carnegie Institution of Washington, Washington, DC 20015, USA*

(Received 7 November 2016; published 30 January 2017)

HPSTAR  
333-2017

$\text{SrCoO}_{2.5}$  has a long-range oxygen vacancy ordering that makes it a promising energy material and catalyst carrier. The study of its electronic properties is vital for its practical applications. Here, we investigate its electronic behavior and lattice structural evolution under high pressure up to 22 GPa using synchrotron infrared spectroscopy and x-ray diffraction. A clear electronic transition from a semiconducting state to another semiconducting state is observed around 7.3 GPa upon compression, based on infrared results. Detailed structural examination shows that this electronic transition is accompanied by a structural phase transition, which occurs between 5.3 and 8.6 GPa, as confirmed by x-ray diffraction. The band gap reduces by  $\sim 40\%$  at high pressure compared to ambient conditions. This work demonstrates that the oxygen vacancy ordering in  $\text{SrCoO}_{2.5}$  can be sustained up to  $\sim 8.6$  GPa and pressure can narrow the band gap, forcing this unique material to enter into another electronic state with a new crystal structure.

DOI: [10.1103/PhysRevB.95.024115](https://doi.org/10.1103/PhysRevB.95.024115)

## I. INTRODUCTION

Vacancy defects provide active centers where chemical reactions can easily start due to local unbalanced charge distribution [1–3]. Furthermore, some vacancy defects are capable of storing small molecules or ions, which is very useful for energy storage and transfer [4–6]. The vacancies in diamond and silicon have provided a proper system for scientists to control spins or spin qubits, an important research discipline in applied (quantum) physics and computer science, or so-called “quantum computation and communication” [7–11].

Vacancies can even form a superstructure with long-range ordering rather than disordered distribution, which makes them much more attractive in the fields of catalyst chemistry and energy conversion.  $\text{SrCoO}_{2.5}$  is one such type of material and it has a long-range order formed by an oxygen vacancy. Currently, there are few reports on the structural change and chemical performance when oxygen atoms enter  $\text{SrCoO}_{2.5}$  and become  $\text{SrCoO}_{3-x}$  [12,13]. Le Toquin *et al.* studied the dynamic process of oxygen intercalation into  $\text{SrCoO}_{2.5}$  via neutron scattering and x-ray absorption spectroscopy. Two intermediate states,  $\text{SrCoO}_{2.75}$  and  $\text{SrCoO}_{2.82}$ , were observed when the oxygen vacancy rate decreased and  $\text{SrCoO}_{2.82}$  showed clear superstructure reflections from the three-dimensional oxygen ordering. Their work shows clear evidence that  $\text{SrCoO}_{2.5}$  has a strong oxygen intercalation capability [14]. Jeon *et al.* reported the reversible redox behavior of  $\text{SrCoO}_{2.5}$  and  $\text{SrCoO}_{3-x}$  epitaxial thin films. The structures of these two phases were tuned using a simple heat treatment near 200–300 °C. They tested the CO-CO<sub>2</sub> redox reaction using  $\text{SrCoO}_{2.5}$  thin film around 320 °C and found that  $\text{SrCoO}_{2.5}$  could be a good redox catalyst for a carbon monoxide oxidation reaction [15].

To explore and extend the potential application of  $\text{SrCoO}_{2.5}$  in chemical engineering, gas sensors, and energy storage, the study of its electronic and structural behavior is crucial. Here, we investigated this unique material using high-pressure infrared spectroscopy and x-ray diffraction. The diamond anvil cell (DAC) based high-pressure method is a useful and clean tool to change crystal structures and their corresponding physical and/or chemical properties [16–18]. Typical examples of this are solid hydrogen and water, which undergo several phase transitions at room temperature under high pressure, extending our basic understanding of chemistry and physics [19–22]. The electronic behavior of  $\text{SrCoO}_{2.5}$  under high pressure was examined using synchrotron infrared microspectroscopy. Our results show that there is an electronic transition from a semiconducting state to another semiconducting state near 7.3 GPa. To understand the mechanism of this transition, the crystal structure was systematically studied based on synchrotron x-ray diffraction. A structural phase transition was observed between 5.3 and 8.6 GPa, confirming the structural origin of the electronic transition. Furthermore, the compressibility of the low-pressure phase showed quasi-isotropic behavior even when the oxygen vacancy order had a strong preferred orientation.

## II. EXPERIMENTS

The  $\text{SrCoO}_{2.5}$  sample was synthesized using a solid-state reaction method. A pellet made from stoichiometric amounts of  $\text{SrCO}_3$  (Sigma-Aldrich 99.9%) and  $\text{Co}_3\text{O}_4$  (Sigma-Aldrich 99.9%) powders was calcined at 1000 °C for 3 days. The sample was then quenched in liquid nitrogen from this temperature. The infrared experiment was performed at the U2A infrared microspectroscopy beamline at the National Synchrotron Light Source (NSLS), Brookhaven National Laboratory. For the infrared study, 300-micron culet-type Ila diamonds were used and transmission mode measurements were employed to investigate its optical behavior. A steel

\*yuebb@hpstar.ac.cn

†chenbin@hpstar.ac.cn

gasket was used and a 100-micron sample chamber was drilled by electrical discharge machining (EDM) provided at the U2A beamline. A thin  $\text{SrCoO}_{2.5}$  sample was placed inside the sample chamber with KBr as a pressure medium. The sample only covered half of the sample chamber and background signals were collected at each pressure point from the other KBr-only half. Two  $40 \times 40$  micron apertures were used to limit the beam size (upstream apertures were placed in front of the diamond anvil cell so infrared light traveled through the aperture first and then arrived at the sample) and exclude environmental light scattering (downstream apertures were placed behind the diamond anvil cell after light traveled through the sample). Seagle *et al.* used a similar setup but only used one aperture [23]. The high-pressure structural evolution was examined by micro x-ray diffraction at beamline 12.2.2 of the Advanced Light Source (ALS) in Lawrence Berkeley National Laboratory and silicon oil was used as a pressure medium. The incident x-ray energy was 25 keV, the wavelength was  $0.4959 \text{ \AA}$ , and the beam size was  $30 \times 30 \mu\text{m}$ . The diffraction patterns were collected from a Mar345 image plate. The pressure was monitored by the Ruby R1-R2 line shift during both the infrared and x-ray diffraction studies [24–26].

### III. RESULTS AND DISCUSSION

The  $\text{SrCoO}_{2.5}$  sample showed a pale black color due to its strong absorption of visible light, which made studying structural changes under high pressure difficult using Raman spectroscopy. No Raman-active modes other than a noisy spectrum were observed. To avoid this problem, we employed infrared spectroscopy to study both the electronic properties and possible structural change of  $\text{SrCoO}_{2.5}$  under high pressure. The use of a synchrotron infrared light source allowed efficient collection of good quality spectra with a relatively low signal to noise ratio. Figure 1 displays a series of absorption spectra at some characterized pressure points. The fluctuating absorption near 0.25 eV is due to the diamond absorption background, which was hard to remove completely during the experiment. A wide peak reveals another diamond absorption region near 0.42 eV. At low pressure, the absorbance in the higher energy range was relatively strong compared with the lower energy region. As pressure increased, the absorbance increased over the whole energy range. A distinctively different absorption spectrum was found at 7.3 GPa: absorbance was significantly enhanced below 0.8 eV, suggesting an electronic phase transition. Higher pressure did not change the energy-dependent absorbance trend and no further qualitative change in the absorption spectra occurred up to the highest investigated pressure.

The band gap was obtained by fitting the absorption spectra with the Tauc relation [27]. Theoretical calculations predicted that  $\text{SrCoO}_{2.5}$  is a semiconductor with an indirect band gap [28]. However, our fitting results suggest a direct band gap. We also tried to fit the spectra using an indirect band gap model but the fitting results made no sense. It should be noted that a  $Pnma$  space group, rather than the mostly accepted  $Imma$  space group, was used in previous calculations [28], which may not provide the accurate result. Hence, further theoretical work is still required. Figure 2 shows the fitting results. The band gap decreased monotonically with pressure

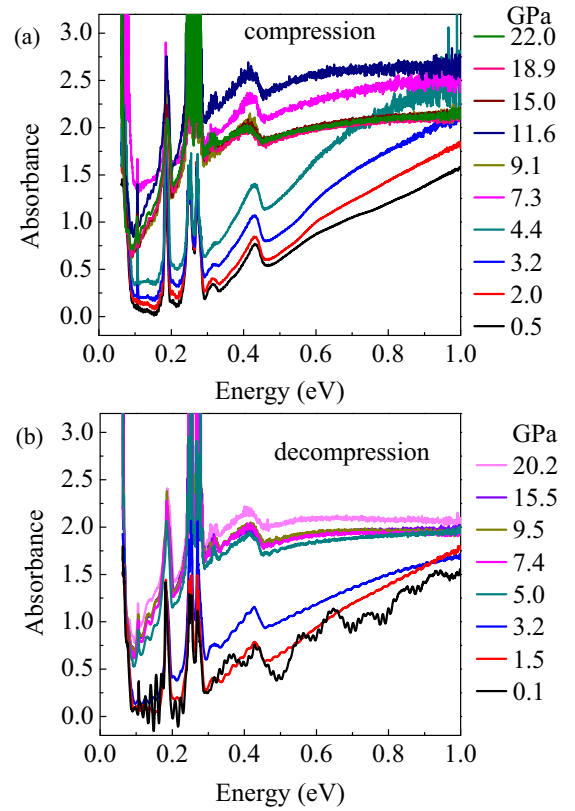


FIG. 1. The infrared absorption spectra of  $\text{SrCoO}_{2.5}$  at selected pressure points: (a) compression and (b) decompression.

up to 10 GPa and did not change much above this pressure during compression. Band gaps were also obtained during decompression and followed a similar trend. In the 0–7.3 GPa pressure range, there was only a small discrepancy between compression and decompression, due to the pressure hysteresis effect. The band gap reduced by  $\sim 40\%$  at 7.3 GPa, compared

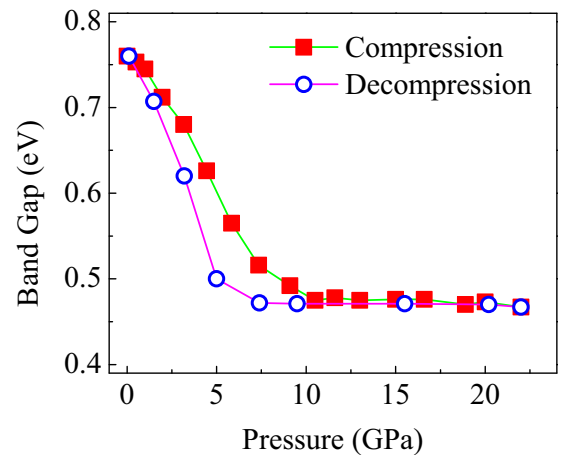


FIG. 2. The pressure-dependent band gap obtained from the Tauc relation  $(\alpha h\nu)^2 = A(h\nu - E_g)$ , where  $\alpha$  is the absorption coefficient,  $h\nu$  is the photoenergy, and  $E_g$  is the band gap. There is a clear electronic phase transition near 7.3 GPa. Above this critical pressure, the band gap value is almost constant but shows negative pressure dependence below 7.3 GPa.

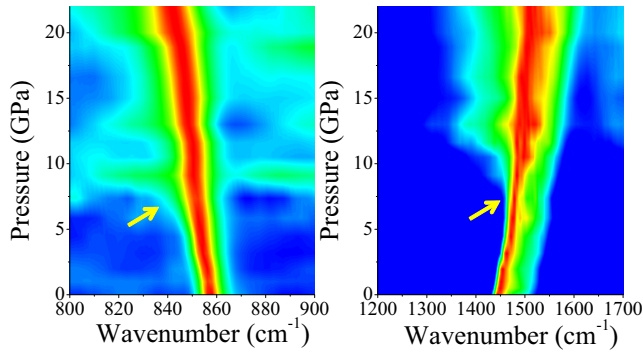


FIG. 3. Infrared-active modes extracted from the absorption spectra. The broadening of the infrared peaks above  $\sim 7.3$  GPa is interpreted as a signature of a phase transition.

with ambient conditions. Considering the band gap trend during these two processes, we conclude that there is an electronic phase transition near 7.3 GPa. The electronic band gap of the low-pressure phase was easily tuned by pressure, while the band gap of the high-pressure phase showed no pressure-dependent behavior in our current pressure range.

This electronic phase transition is also confirmed by the damping behavior of two infrared-active vibration modes. Figures 3 and 1 show two sharp peaks in the low-energy region around 0.1–0.2 eV. At ambient conditions, the first peak near  $860\text{ cm}^{-1}$  (equal to 0.107 eV) is relatively weak and the second near  $1450\text{ cm}^{-1}$  (equal to 0.181 eV) is stronger. These two IR-active vibration modes are assigned to the  $\nu_2$  mode (in-plane bending of the  $\text{CoO}_6$  octahedron) and the  $\nu_3$  mode (asymmetric stretching of the Co-O bond), which are similar to those observed in  $\text{SrCoO}_3$  [29,30]. The low-frequency mode redshifts under high pressure and the high-frequency mode blueshifts. Above  $\sim 7.3$  GPa, both consistently start to broaden. The damping effect is very strong above 10 GPa, especially for the high-frequency mode.

In order to reveal the origin and mechanism of the electronic phase transition, the lattice structural evolution under high pressure was examined *in situ* by synchrotron x-ray microdiffraction. The pressure-dependent XRD pattern is shown in Figs. 4(a) and 4(b). At ambient conditions, the sample shows a pure brownmillerite phase with space group  $Imma$  [Fig. 4(c)]. When the pressure increased, all diffraction peaks shifted to a higher angle, suggesting that the lattice parameter and volume also contracted. Between 5.3 GPa and 8.6 GPa, some peaks were strongly suppressed indicating a structural phase transition, which is well matched with the electronic phase transition pressure determined by the infrared absorption spectra. The peak ( $2\theta \approx 3.6^\circ$ ) contributed by the oxygen vacancy ordering was also suppressed above this critical phase transition pressure. Hence, the structure of  $\text{SrCoO}_{2.5}$  was stable up to  $\sim 8.6$  GPa. Above this transition pressure, DicVol04 software assigns the structure to another orthorhombic structure with space group  $P222$ . However, this high-pressure phase is somewhat difficult to determine due to the weak and broadened diffraction signal. According to previous calculations, the structure with space group  $Pnma$  is possibly a low-temperature phase for  $\text{SrCoO}_{2.5}$  and sometimes effects of high pressure on the crystal structure are qualitatively comparable to those

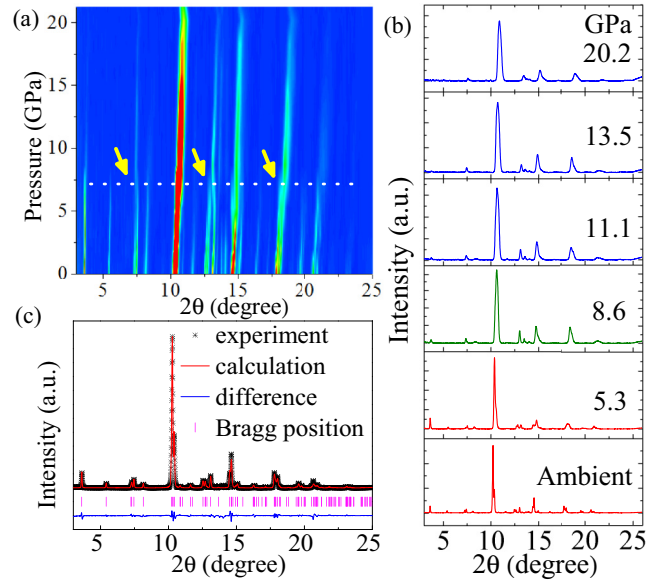


FIG. 4. Pressure-dependent x-ray diffraction patterns. (a) 2D XRD pattern; yellow arrows are plotted to show the phase transition. (b) Selected XRD patterns at various pressures (ambient conditions, 5.3 GPa, 8.6 GPa, 11.1 GPa, 13.5 GPa, and 20.2 GPa). (c) XRD refinement (ambient conditions).

induced by low temperature. Similar systems, such as  $\text{CaFeO}_{2.5}$ , can exist in the form of a  $Pnma$  structure [28,31]. Therefore, it is possible that the high-pressure phase has a  $Pnma$  structure. However, based on the peak position information, the only possible structure is  $P222$  rather than  $Pnma$  and other orthorhombic structures. We also considered the possibility of a cubic phase, which is the stable structure found in  $\text{SrCoO}_3$  [32]. However, the cubic phase was finally excluded due to the large mismatch of the Bragg positions, despite their patterns looking quite similar. Further study is still required to clarify the structural details in the high-pressure phase.

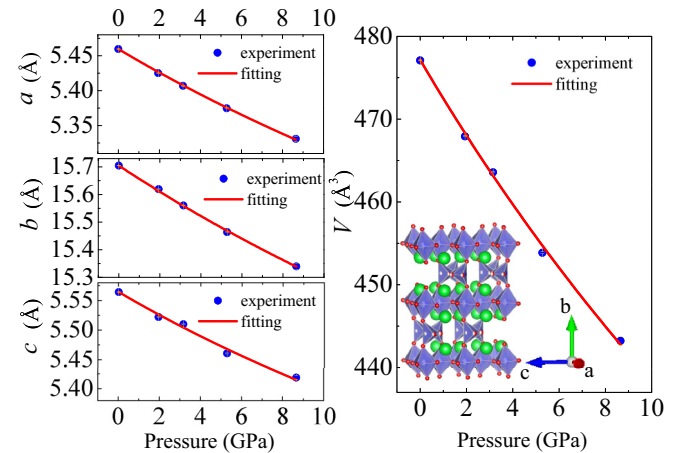


FIG. 5. The lattice parameter and volume change under high pressure for the low-pressure phase. Both the lattice parameters and volume decrease monotonically with pressure. The compressibilities of  $a$ ,  $b$ , and  $c$  are very similar and there is no clear anisotropic dependence. Inset: The atomic structure of  $\text{SrCoO}_{2.5}$ .

To further test the structural stability of the brownmillerite phase, the compressibility was examined by comparing the pressure-dependent lattice parameters along the  $a$ ,  $b$ , and  $c$  directions. The results are presented in Fig. 5 and the volume change is also presented for reference. All three lattice parameters show a similar trend with pressure. Birch-Murnaghan equation of state (EOS) analysis ( $K' = 4.0$ , fixed) gives the linear modulus:  $K_a = 103.6 \pm 9.6$  GPa,  $K_b = 106.1 \pm 9.8$  GPa, and  $K_c = 90.9 \pm 8.4$  GPa. Hence, there is no strong anisotropic compressibility behavior. The bulk modulus is  $K_B = 99.9 \pm 9.3$  GPa ( $K'_B = 4.0$ , fixed). This suggests that the lattice structure of the oxygen vacancy ordered  $\text{SrCoO}_{2.5}$  is very stable and shows quasi-isotropic compressibility in the low-pressure range from ambient conditions to  $\sim 7.3$  GPa (confirmed by IR and XRD experiments). At 8.6 GPa, the structure became unstable.

#### IV. CONCLUSION

The electronic and structural behavior of  $\text{SrCoO}_{2.5}$  under high pressure was investigated by synchrotron infrared microspectroscopy and x-ray diffraction. The infrared spectroscopy experiment revealed an electronic transition from a semiconducting state to another semiconducting state near 7.3 GPa. The XRD-based structural investigation showed a structural phase transition between 5.3 and 8.6 GPa, which suggests the observed electronic transition had a structural origin. In the low-pressure phase, the band gap decreased when the pressure increased. For the high-pressure phase,

the band gap had weak pressure dependence. In addition, the lattice parameters of the low-pressure phase showed unexpected quasi-isotropic compressibility, which could be advantageous for its application in the fields of energy storage, catalyst carriers, and gas sensors at both ambient and extreme conditions.

#### ACKNOWLEDGMENTS

The authors acknowledge support from the NSAF (Grant No. U1530402). F.H. and B.B.Y. acknowledge the usage of beam time at beamline U2A at the National Synchrotron Light Source and beam time at beamline 12.2.2 at the Advanced Light Source, Lawrence Berkeley National Laboratory. The use of the U2A beamline at the National Synchrotron Light Source was supported by COMPRES under NSF Cooperative Agreement No. EAR 11-57758 and CDAC (DE-FC03 03N00144). The National Synchrotron Light Source, Brookhaven National Laboratory, was supported by the US Department of Energy, Office of Science, Office of Basic Energy Sciences, under Contract No. DE-AC02-98CH10886. The Advanced Light Source is supported by the Director, Office of Science and Office of Basic Energy Sciences, US Department of Energy, under Contract No. DE-AC02-05CH11231. Partial work was supported by COMPRES (the Consortium for Materials Properties Research in Earth Sciences) under NSF Cooperative Agreement No. EAR 10-43050. All authors thank Freyja O'Toole for her careful revision of the manuscript.

- 
- [1] X. Liu, K. Zhou, L. Wang, B. Wang, and Y. Li, *J. Am. Chem. Soc.* **131**, 3140 (2009).
  - [2] H. Gunaydin, K. N. Houk, and V. Ozoliņš, *Proc. Natl. Acad. Sci. USA* **105**, 3673 (2008).
  - [3] Z. A. Feng, F. El Gabaly, X. Ye, Z.-X. Shen, and W. C. Chueh, *Nat. Commun.* **5**, 5374 (2014).
  - [4] X. Li, Y. Feng, M. Li, W. Li, H. Wei, and D. Song, *Adv. Funct. Mater.* **25**, 6858 (2015).
  - [5] F. T. Li, J. Ran, M. Jaroniec, and S. Z. Qiao, *Nanoscale* **7**, 17590 (2015).
  - [6] Y. Xu, M. Zhou, X. Wang, C. Wang, L. Liang, F. Grote, M. Wu, Y. Mi, and Y. Lei, *Angew. Chem. Int. Ed.* **54**, 8768 (2015).
  - [7] C. G. Yale, F. J. Heremans, B. B. Zhou, A. Auer, G. Burkard, and D. D. Awschalom, *Nat. Photonics* **10**, 184 (2016).
  - [8] H. Kosaka and N. Niikura, *Phys. Rev. Lett.* **114**, 053603 (2015).
  - [9] S. Kolkowitz, A. Safira, A. A. High, R. C. Devlin, S. Choi, Q. P. Unterreithmeier, D. Patterson, A. S. Zibrov, V. E. Manucharyan, H. Park, and M. D. Lukin, *Science* **347**, 1129 (2015).
  - [10] J. J. Pla, K. Y. Tan, J. P. Dehollain, W. H. Lim, J. J. L. Morton, F. A. Zwanenburg, D. N. Jamieson, A. S. Dzurak, and A. Morello, *Nature (London)* **496**, 334 (2013).
  - [11] J. J. Pla, K. Y. Tan, J. P. Dehollain, W. H. Lim, J. J. L. Morton, D. N. Jamieson, A. S. Dzurak, and A. Morello, *Nature (London)* **489**, 541 (2012).
  - [12] H. Jeon, W. S. Choi, J. W. Freeland, H. Ohta, C. U. Jung, and H. N. Lee, *Adv. Mater.* **25**, 3651 (2013).
  - [13] H. Jeon, Z. Bi, W. S. Choi, M. F. Chisholm, C. A. Bridges, M. P. Paranthaman, and H. N. Lee, *Adv. Mater.* **25**, 6459 (2013).
  - [14] R. Le Toquin, W. Paulus, A. Cousson, C. Prestipino, and C. Lamberti, *J. Am. Chem. Soc.* **128**, 13161 (2006).
  - [15] H. Jeon, W. S. Choi, M. D. Biegalski, C. M. Folkman, I. C. Tung, D. D. Fong, J. W. Freeland, D. Shin, H. Ohta, M. F. Chisholm, and H. N. Lee, *Nat. Mater.* **12**, 1057 (2013).
  - [16] F. Hong, B. Yue, Z. Cheng, M. Kunz, B. Chen, and H.-K. Mao, *Appl. Phys. Lett.* **109**, 041907 (2016).
  - [17] F. Hong, B. Yue, N. Hirao, G. Ren, B. Chen, and H.-K. Mao, *Appl. Phys. Lett.* **109**, 241904 (2016).
  - [18] B. Yue, F. Hong, S. Merkel, D. Tan, J. Yan, B. Chen, and H.-K. Mao, *Phys. Rev. Lett.* **117**, 135701 (2016).
  - [19] C. S. Zha, R. E. Cohen, H. K. Mao, and R. J. Hemley, *Proc. Natl. Acad. Sci. USA* **111**, 4792 (2014).
  - [20] B. Kamb and B. L. Davis, *Proc. Natl. Acad. Sci. USA* **52**, 1433 (1964).
  - [21] I.-M. Chou, J. G. Blank, A. F. Goncharov, H.-k. Mao, and R. J. Hemley, *Science* **281**, 809 (1998).
  - [22] C. Lobban, J. L. Finney, and W. F. Kuhs, *Nature (London)* **391**, 268 (1998).
  - [23] C. T. Seagle, D. L. Heinz, Z. Liu, and R. J. Hemley, *Appl. Opt.* **48**, 545 (2009).
  - [24] H. K. Mao and P. M. Bell, *Science* **191**, 851 (1976).
  - [25] J. H. Eggert, K. A. Goettel, and I. F. Silvera, *Phys. Rev. B* **40**, 5724 (1989).
  - [26] J. H. Eggert, K. A. Goettel, and I. F. Silvera, *Phys. Rev. B* **40**, 5733 (1989).



- [27] J. Tauc and A. Menth, *J. Non-Cryst. Solids* **8-10**, 569 (1972).
- [28] H.-P. Wu, K.-M. Deng, F.-L. Hu, W.-S. Tan, C.-M. Tang, and Q.-X. Li, *Chin. Phys. Lett.* **26**, 017105 (2009).
- [29] B. Sreedhar, M. Sulochana, C. S. Vani, D. K. Devi, and N. V. S. Naidu, *Eur. Chem. Bull.* **3**, 234 (2014).
- [30] S. Makhloufi and M. Omari, *J. Inorg. Organomet. Polym.* **26**, 32 (2016).
- [31] M. I. Gómez, J. A. de Morán, R. E. Carbonio, and P. J. Aymonino, *J. Solid State Chem.* **142**, 138 (1999).
- [32] J. Y. Yang, C. Terakura, M. Medarde, J. S. White, D. Sheptyakov, X. Z. Yan, N. N. Li, W. G. Yang, H. L. Xia, J. H. Dai, Y. Y. Yin, Y. Y. Jiao, J. G. Cheng, Y. L. Bu, Q. F. Zhang, X. D. Li, C. Q. Jin, Y. Taguchi, Y. Tokura, and Y. W. Long, *Phys. Rev. B* **92**, 195147 (2015).